

- ¹J. W. Conolly, *Phys. Rev.* **159**, 415 (1967).
²S. Wakoh and J. Yamashita, *J. Phys. Soc. Jpn.* **28**, 1151 (1970).
³S. Ishida, *J. Phys. Soc. Jpn.* **33**, 369 (1973).
⁴I. Rosenman and F. Batallan, *Phys. Rev.* **135**, 1340 (1972).
⁵P. Heimann, E. Marschall, H. Neddermeyer, M. Pessa, and H. F. Roloff, *Phys. Rev. B* **16**, 2575 (1977).
⁶F. Batallan, I. Rosenman, and C. B. Sommers, *Phys. Rev. B* **11**, 545 (1975).
⁷C. M. Singal and T. P. Das, *Phys. Rev. B* **16**, 5068 (1977).
⁸E. P. Wohlfarth, *J. Appl. Phys.* **41**, 1205 (1970).
⁹A. P. Lenham and D. M. Treherne, in: *Optical Properties and Electronic Structure of Metals and Alloys*, Amsterdam, 1966, p. 196.
¹⁰M. M. Kirillova and B. A. Charikov, *Opt. Spektrosk.* **17**, 254 (1964).
¹¹L. A. Afanas'eva and M. M. Kirillova, *Fiz. Met. Metalloved.* **23**, 472 (1967).
¹²G. A. Bolotin, M. M. Noskov, and I. I. Sasovskaya, *Fiz. Met. Metalloved.* **35**, 699 (1973).
¹³G. S. Krinchik and V. S. Gushchin, *Zh. Eksp. Teor. Fiz.* **56**, 1833 (1969) [*Sov. Phys. JETP* **29**, 984 (1969)].
¹⁴G. S. Krinchik and E. A. Gan'shina, *Zh. Eksp. Teor. Fiz.* **65**, 1970 (1973) [*Sov. Phys. JETP* **38**, 983 (1973)].
¹⁵G. S. Krinchik and G. M. Nurmukhamedov, *Zh. Eksp. Teor. Fiz.* **48**, 34 (1964) [*Sov. Phys. JETP* **21**, 22 (1964)].
¹⁶I. L. Erskine and E. A. Stern, *Phys. Rev. B* **8**, 1239 (1974).
¹⁷E. Fawcett and W. A. Reed, *Phys. Rev. Lett.* **9**, 336 (1962).
¹⁸J. O. Dimmock, A. J. Freeman, and R. E. Watson, in: *Optical Properties and Electronic Structure of Metals and Alloys*, Amsterdam, 1966, p. 237.
¹⁹C. S. Wang and J. Callaway, *Phys. Rev. B* **9**, 4897 (1974).
²⁰M. Singh, C. S. Wang, and J. Callaway, *Phys. Rev. B* **11**, 287 (1975).

Translated by J. G. Adashko

Unloading isentropes and the equation of state of metals at high energy densities

L. V. Al'tshuler, A. V. Bushman, M. V. Zhernokletov, V. N. Zubarev, A. A. Leont'ev, and V.E. Fortov

All-Union Research Institute of Optical-Physics Measurements
 (Submitted 19 July 1979)
Zh. Eksp. Teor. Fiz. **78**, 741-760 (February 1980)

The release (unloading) isentropes of shock-compressed samples of copper and lead are experimentally investigated in a wide range of thermodynamic parameters, from states on the shock adiabat ($R-H$ curves) at a pressure 0.5-2.5 Mbar to near-critical states. The investigations make it possible to determine the thermodynamics and to ascertain the form of the phase diagram in this region. An interpolation equation of state is derived to describe the behavior of metals on the entire phase plane, with allowance for high-temperature melting and evaporation. The coefficients of the equations of state are determined and the thermodynamic characteristics of copper and lead are calculated from the results of the experiments and from other experimental and theoretical information.

PACS numbers: 64.30. + t, 65.50. + m

1. INTRODUCTION

The methods developed by now to apply intense pulses on metals (lasers, electron beams, ion and neutron beams, powerful shock and electromagnetic waves¹) produce in the condensed phase a high local energy concentration exceeding the binding energy, so that a plasma with a strong interparticle interaction is formed. For an adequate description of the physical processes and the motion dynamics in action of this kind it is necessary to know the thermodynamic properties of the material in a wide range of pressures and temperatures, covering the entire spectrum of the states that arise in pulsed energy release. It is particularly important to take a detailed account of the high-temperature melting and evaporation, and to describe correctly the characteristics of the metals under conditions of disorder and great deviation from the ideal state.

An arbitrary phase diagram of a metal is shown in Fig. 1, where the regions that can be treated theoretically and experimentally are marked schematically.

The modern theoretical methods are valid in the limit of extremal high pressures and temperatures, where one can use the quasiclassical (the Thomas-Fermi theory with corrections²-TFC) and the classical (the Debye-Huckel³) approximations of the self-consistent

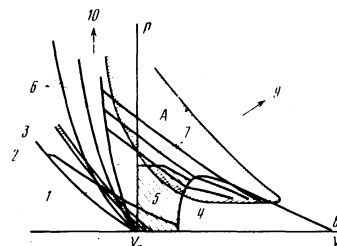


FIG. 1. Arbitrary phase diagram of metal. 1—static experiments, 2—isootherm $T=293$ K, 3—melting region, 4—liquid-vapor equilibrium curve, 5—exploding-wire method, 6—experimental shock adiabats, 7—release isentropes, 8—ideal gas, 9—ideal plasma, 10—Thomas-Fermi electron gas; A—uninvestigated region with strong interparticle interaction. The arrows point to a decrease of the nonideality parameter.

field, with a correct approach to the behavior of an ideal gas. With decreasing pressures and temperatures, the effectiveness of these models decreases because of the difficulties encountered in the quantum-mechanical description of the interparticle interaction, which is strong and of complicated structure, and calls for knowledge of the actual band or shell structure of the element. Therefore, despite the interesting qualitative results obtained for metals using the Wigner-Seitz quantum-mechanical model,⁴ and obtained for a plasma in a liquid within the framework of the pseudopotential model⁵ and the "hard" and "soft" sphere models,⁶ the main source of quantitative information in a strongly nonideal region of the parameters is experiment.

Stationary thermophysical experiments have made it possible to ascertain for most metals the form of the phase diagram and to find the thermodynamic characteristics of the solid and liquid phases in the range of pressures $P < 50$ kbar and temperatures $T < 2500$ K.^{7,8} The use of internal pressure standards has expanded the region of the static investigations aimed at determining the isothermal compressibility and the form of the phase diagram up to 1 Mbar.⁹ The standard compression curves of several metals (Cu, Mo, Pd, Ag), which are needed for this purpose, were calculated with good approximation from the results of dynamic experiments with the aid of shock waves.¹⁰

The large binding energy and accordingly the high values of the critical parameters of metals restrict greatly the capabilities of stationary experiments near the liquid-vapor phase-equilibrium line. Up to now, a complete investigation of the near-critical region was made only for the metals with the lowest boiling points—cesium¹¹ and mercury.¹² New advances were made in recent years in the method of exploding wires. By performing the experiments in compressed helium it became possible to register simultaneously in the metals, at a pressure of several kbar, the specific volume, the enthalpy, and the temperature in the range up to 5000 K.¹³

The use of strong shock waves in high-pressure physics¹⁴ has made it possible to investigate, using experiments on shock compression of solid and porous samples, the region of the condensed phase of metals up to pressures ~ 10 Mbar and temperatures of tens of thousands of degrees.^{15,16} Succeeding experiments extended the region of dynamic measurements to several dozen megabars and hundreds of thousands of degrees. Under these experimental conditions, the relative compressibilities of iron, lead, copper, and cadmium were determined¹⁷ and the first absolute measurements were made of the pressure and the density of molybdenum.¹⁸ Significant information for the derivation of the equation of state at high energy densities is obtained by determining the course of the dynamic adiabats of highly porous copper up to 20 Mbar.¹⁹ The specifics of shock-wave studies make it possible to register only the calorific characteristics of a medium—pressure, specific volume, and energy—but not the temperature or the entropy. However, the entropy on the shock adiabats can be determined from the parameters of the final state of

the metal following its adiabatic expansion. Limited but very important entropy information was obtained by determining the residual temperatures of the expansion of copper in air²⁰ and from spectroscopic measurements of the fraction of metal (Li, Na, Ba, Sr, U) evaporated in vacuum when the pressure was released.²¹ The evaporation of shock-compressed lead following release in air was investigated in Ref. 22. This made it possible, by determining the start of the evaporation, to obtain for one of the isentropes the parameters of its entry into the two-phase region and to estimate the entropy of the metal from the shock adiabat.

It is seen from the foregoing review of the existing methods of theoretically describing and experimentally investigating the thermodynamic properties of metals that the extensive region *A* of the phase diagram of Fig. 1, which is of practical importance, has not yet been investigated. Complicated physical processes are realized in this medium: degeneracy of the electronic component and its recombination in a heated metallic liquid that is nonideal with respect to a broad spectrum of interparticle interactions when the liquid expands, a metal-insulator transition, and high-temperature evaporation into the gas or plasma phase. The lack of reliable experimental and theoretical information on the strongly nonideal region of parameters has given rise a great variety of hypotheses that require experimental verification. In particular, under active discussion is at present the question of the exotic phase transitions of first and second order which are due to metallization of vapors,²³ as well as to the strong collective interaction of charges with charges,^{5,24} with neutrals,²⁵ and with clusters.²⁶

In the present study we have investigated the properties of copper and lead in region *A* by a dynamic method based on the study of the isentropes of the expansion of a metal that is compressed and is irreversibly heated in the front of a powerful shock wave.²⁷ Successive registration of the rates of expansion at various release pressures determines, by means of the known Riemann differential relations, the change of the specific volume and the energy of the expanding metal. A similar approach in the study of uranium and copper was partially realized in Refs. 28 and 29, but the interpretation of the results described in these papers was made difficult by the large scatter and incompleteness of the experimental data, especially at low pressures.

In our investigation, the isentropic expansion method was realized to the fullest extent by detailed registration of the release states at various initial entropies. The high-energy states were attained by using powerful propulsion systems energized by detonation of condensed explosives. To increase further the effects of dissipation in the shock-wave front, the copper and lead samples were made of finely dispersed powder. The use of shock waves with different intensities and of a large number of condensed and gas barriers, made it possible to determine the hydrodynamic and thermodynamic characteristics of the expansion process and to ascertain the shape of the phase diagram of the investigated metals in a wide range of continuously varying

parameters.

The results of the investigation (reported by us in part earlier^{30,31}) and other calculated and experimental data on the thermodynamic properties of copper and lead were unified within the framework of a semi-empirical model equation of state. The type of potential chosen for the description has a physically well-founded form of individual terms and a number of free fit parameters. Equations of state of this type^{15,16,32,33} were used earlier to calculate the characteristics of the condensed phases of metals. Wide-range equations of state^{34,35} have a rigidly specified model potential and take no account in practice of the experimental results. An approximate description³⁶ that takes into account the aggregate of experimental and calculated data in a large section of the phase plane does not yield correct asymptotic relations and does not account for the small-scale phenomena (melting, ionization, etc.). The derived equations have made it possible to expand the region of description and to determine the thermodynamics of solid, liquid, gas, and plasma states with explicit separation of all the asymptotic forms and with account taken of the high-temperature melting and evaporation; the use of new experimental data made it possible to describe the properties of the high-energy states of copper and lead with high reliability and completeness.

2. ISENTROPIC-EXPANSION METHOD. RESULTS OF EXPERIMENT

A schematic diagram of the method of isentropic expansion is shown in Fig. 2. A high-power shock wave propagating along the investigated substance M compresses the latter and causes it to be irreversibly heated to a state a . The emergence of the shock wave to its border Bo with a dynamically softer barrier Ba results in the production of a centered Riemann wave C^+C^- , in which the shock-compressed matter expands adiabatically from the state a to the state i . This expansion of the metal produces in the barrier a shock wave that propagates with velocity D_i . By recording D_i it is possible, knowing the shock adiabat h_i , to determine the pressure P_i and the mass velocity U_i of the barrier, which by virtue of the continuity²⁷ on the contact boundary Bo coincide with the corresponding characteristics of the expanding metal.

Using barriers with differing dynamic rigidity and recording the produced P and U , it is possible to trace

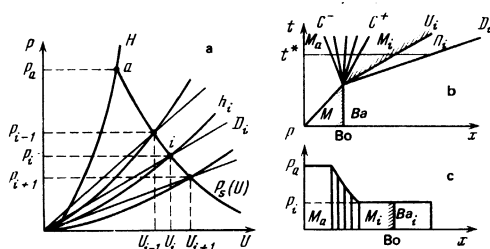


FIG. 2. Isentropic expansion method: a) $P-U$ diagram of experiments, b) $x-t$ diagram, c) $x-T$ diagram for the instants of time t^* .

continuously the expansion isentrope $P = P_s(U)$ from states on the Hugoniot adiabat to near-critical values and temperatures. The use of propulsion systems of varying power makes it possible to vary the entropy in the shock wave and by the same token investigate various isentropes that cover the chosen region of the phase diagram. The transition from hydrodynamic variables (P, U) to the thermodynamic variables (P, V, E) can be effected by calculating the Riemann integrals that express the conservation laws for a given type of self-similar flow²⁷:

$$V_i = V_a - \int_{P_a}^P \left(\frac{dU}{dP} \right)^2 dP, \quad E_i = E_a + \int_{P_a}^P \left(\frac{dU}{dP} \right)^2 dP. \quad (1)$$

To choose the optimal conditions of the dynamic experiment, we calculated those states of copper and lead in the region of the condensed phase, whose decay of leads to evaporation or condensation in the release wave.³⁷ We use initially estimates of the parameters of the critical point³⁸ and calculations of the shock adiabats using an equation of state of the type considered in Ref. 33. Figure 3 shows the shock-compression entropies, calculated from the equation of state of the present paper (see Sec. 3), of samples of copper and lead of different porosity, as well as the states produced when an iron flyer plate moving with specified velocity is stopped by the investigated substances.

It is seen from Fig. 3 that dynamics generation methods make it possible to realize high-energy states of metals in a wide range of parameters near the liquid-vapor equilibrium line. To attain transcritical conditions in the release wave, however, it is necessary to have generators of shock waves of extremely high intensity, at the limits of the capabilities of chemical explosives. The necessary shock-wave amplitudes could be substantially decreased by using porous targets, which ensure a more effective increase of the shock-compression entropy. This raises at the same time methodological questions connected with the influence of the structure of porous samples on the measurement results.

The condition that local thermodynamic equilibrium be produced imposes a limitation on the sample grain size, in view of the requirement that the particles be completely heated during the time of the dynamic ex-

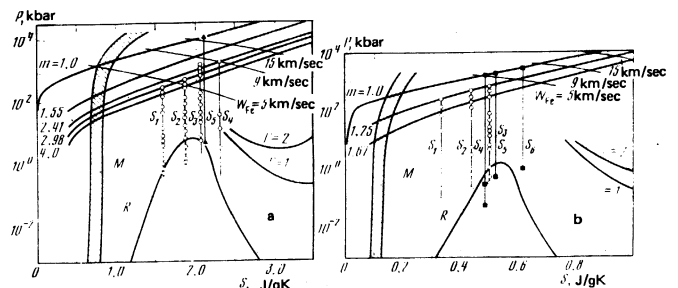


FIG. 3. $P-S$ diagram of copper (a) and of lead (b): m —shock adiabats of different porosity, W —states produced in samples when they stop iron strikers with different velocities, S —release isentropes (\circ —the authors' experiment, \triangle —³⁹, \blacksquare —²²), M —melting region, R —liquid-vapor equilibrium region, Γ —Coulomb-nonideality parameter.

periment. The size of the thermal skin layer under the experimental conditions is $\delta = (\lambda/c_p)^{1/2} t \sim 10\text{--}50 \mu\text{m}$, as a result of which the grain diameter was chosen to range from 3 to 10 μm . It should be noted that the condition of complete heating is violated for a narrow layer of metal at the contact border, because of the shorter time of the dynamic action. In the single-phase region this layer exerts practically no influence on the hydrodynamics of the process, because of the invariance of the average volume with respect to local redistribution of the energy.⁴⁰ When the release isentropes approach the liquid-vapor phase boundary from the liquid phase, and as they enter further into the two-phase region, the energy redistribution can, however, cause an excess formation of the gas phase and an additional increase in the expansion rate. An analysis of the distribution of the energy between the porous metal and the gas shock-compressed in its pores shows²⁸ a similar tendency. According to estimates, both indicated factors are significant only at low pressures (on the order of a kilobar), when the influence of the boundary layer of the metal on the hydrodynamics of the expansion or when the masses of the shock-compressed gas and of the expanding metal become commensurate; the effect of these factors increases with increasing porosity of the samples. A series of methodological experiments with variation of the degree of dispersion of the samples from 3 to 50 μm has confirmed that pressures on the order of a kilobar determine the lower limit of the applicability of the isentropic expansion of porous samples.

The bulk of the experiments on isentropic expansion were performed with porous targets of copper ($m = 2.41$ and 2.98) and of lead ($m = 1.25$). Shock waves of various durations and amplitudes were generated by explosive propelling devices whose action was based on acceleration, by the detonation products of condensed explosives, of metallic strikers of varying thicknesses, to a velocity 2–9 km/sec.¹⁴ The dimensions of the targets and of the measurement base were chosen such as to keep the distorting influence of the release waves away from the elements of the experimental assembly and of the explosive propelling system.

The states produced in the release wave were registered by a reflection method.¹⁴ At high dynamic pressures, the obstacles were "soft" condensed media—light metals (Al, Mg), Plexiglas, polyethylene, and polystyrene of varying density. The velocity of the shock wave in the condensed obstacles was measured by a system of electric-contact pickups, with the signals recorded by high-speed oscilloscopes. The parameters of the initial states of the metals were obtained by the reflection method from the measured values of the wave velocities and the known dynamic adiabats of the screens, whose kinematic parameters were determined in a separate series of experiments.

The region of considerable rarefaction and decrease of the dynamic pressures, which is of particular interest because it has been little studied, was reached by using as barriers heavy inert gases (argon and xenon) at pressures 0.1–100 bar, as well as air at atmospher-

ic pressure. The maximum initial gas pressure was chosen such as to reach states close to those attained in the softest condensed obstacles.

In experiment with gas barriers, the kinematic parameters of the shock waves were registered by electric-contact and optical-base methods.⁴¹ In the first of these methods the velocity of the shock-wave front was registered by a system of six electric contacts so arranged as to take into account the possible skewing of the shock-wave front. In the optical measurement methods we scanned the emission of the shock-compressed plasma by using an electron-optical converter or a streak camera. The reference time markers were the start of the emission of the gas upon entry of the shock wave at the target boundary and the change of the emission when the wave struck a transparent barrier mounted at a specified distance from the target. A series of control experiments has shown that the emission begins practically simultaneously with the start of motion of the metal surface.

To determine the dynamic parameters of the low-pressure gas barriers we use results of thermodynamic calculations of the shock adiabats (R-H curves) of argon and xenon, with allowance for multiple ionization, electron excitation, and deviation from ideal Coulomb conditions.⁴² At increased pressures and densities, the reliability of the thermodynamic calculations decreases because of the strong interparticle interaction in the dense plasma. To determine more accurately the dynamic characteristics of the gas partitions, experiments were performed⁴¹ and have shown that a nonideal plasma has a compressibility lower than the calculated value,¹⁾ and this fact was taken into account in the reduction of the experimental data. The simultaneous and independent registration of the wave and mass velocity of shock-compressed plasma, carried out in a number of experiments, has confirmed the accuracy of the correction and the compatibility of the optical and electric-contact procedures.

The experimental results on isentropic expansion of copper and lead are given in Tables I and II, where each experimental point was obtained 3–5 experiments with 4–6 independent readings in each. Table III lists the coefficients of the linear $D-U$ relations ($D = C_{ba} + \lambda_{ba} U$) of the employed barriers and, for gases, the limits of the applicability of the presented relations. In the case of gas barriers, the reduced data were corrected for the change in the ambient air temperature; the data of Tables I and II are referred to an initial barrier temperature $T_0 = 293 \text{ K}$. The experimental points for the expansion isentropes, together with those available from the shock-wave experiment, are marked on Figs. 4 and 5.

3. SEMI-EMPIRICAL EQUATION OF STATE OF A METAL

The derived equation of state of a metal develops the general principles previously expounded in the semi-empirical equations of state of a condensed phase,^{15, 16, 32, 33} namely, representation of the thermodynamic potential by a sum of terms that describe the

TABLE I. Release isentropes of copper.

Barrier	D, km/sec	U, km/sec	P, kbar	Barrier	D, km/sec	U, km/sec	P, kbar
<i>S</i> ₁ , <i>m</i> =2.98				Argon 10	7.55	6.48	8.1
Sample	4.32	2.73	354	Argon 5	7.62	6.55	4.1
Plexiglas	6.96	2.92	240	Argon 3	7.69	6.74	2.6
Polyethylene	7.40	3.09	210	Argon 2	7.92	6.96	1.8
Styrofoam 0.5	5.23	3.46	90	Argon 1.5	8.31	7.34	1.5
Styrofoam 0.3	5.04	3.79	57	Argon 1	8.73	7.75	1.1
Xenon 20	4.46	3.82	18	<i>S</i> ₃ , <i>m</i> =2.41			
Xenon 10	4.61	3.96	10	Sample	7.71	4.84	1380
Xenon 5	4.66	4.00	5.1	Aluminum	11.60	4.64	1460
Xenon 1	4.93	4.39	1.2	Magnesium	11.09	5.31	1020
Argon 20	5.11	4.13	7.0	Magnesium	10.91	5.92	760
Argon 10	5.11	4.13	3.5	Styrofoam 0.66	10.31	6.88	470
Argon 5	5.05	4.08	1.7	Styrofoam 0.3	10.02	7.65	230
Argon 3	5.25	4.37	4.1	Xenon 30	9.70	8.42	160
Argon 2	5.48	4.59	0.83	Xenon 20	9.65	8.38	100
Argon 1.5	5.49	4.60	0.63	Xenon 10	10.39	9.03	54
Argon 1	5.70	4.80	0.45	Xenon 5	10.64	9.25	28
<i>S</i> ₂ , <i>m</i> =2.98				Xenon 1	11.63	10.48	6.7
Sample	5.69	3.68	630	Argon 20	10.77	9.58	34
Plexiglas	8.28	3.92	380	Argon 5	11.18	9.97	9.3
Poyethylene	9.02	4.18	350	Argon 1	12.06	10.98	2.2
Styrofoam 0.5	6.77	4.63	160	<i>S</i> ₄ , <i>m</i> =2.41			
Styrofoam 0.3	6.67	5.05	100	Sample*	9.48	6.04	2120
Xenon 30	6.48	5.60	59	Xenon 5	13.79	12.00	46
Xenon 20	6.54	5.65	41	Argon 5	14.77	13.34	16
Xenon 10	6.90	5.96	22	Argon 1	16.02	14.47	3.8
Xenon 1	7.65	6.86	2.9	Argon 0.36	16.50	14.91	1.5
Argon 20	7.35	6.29	15	Argon 0.1	17.90	16.18	0.46

*Obtained by calculation from the known parameters of the screen in the shock adiabat *m* = 2.41.

contribution of the lattice, of the electrons, etc. At the same time, the concrete form of the individual terms was changed to be able to take into account more correctly the effects of melting, lattice anharmonicity, and electron contributions, and to extend the thermodynamic properties of metals to a larger section of the phase plane. In particular, account was taken of high-temperature evaporation, a correct asymptotic relation was introduced for the terms that characterize the melting, a continuous transition was made from a degenerate to an ideal electron gas, and the effects of the first ionization were taken into account. Introduction into the equation of state of additional terms that describe these effects has led, however, to a corresponding increase of the number of the fit parameters.

The free energy *F*, chosen to be the thermodynamic potential of the solid and liquid phases, consists of

TABLE II. Release isentropes of lead.

Barrier	D, km/sec	U, km/sec	P, kbar	Barrier	D, km/sec	U, km/sec	P, kbar
<i>S</i> ₁ , <i>m</i> =1.25				<i>S</i> ₃ , <i>m</i> =1.25			
Sample	3.09	1.18	331	Sample	4.64	2.22	934
Magnesium	6.49	1.59	180	Aluminum	8.90	2.64	640
Plexiglas	4.95	1.55	91	Magnesium	8.02	2.80	390
Styrofoam 0.5	2.91	1.69	25	Plexiglas	7.05	2.99	250
Argon 20	2.57	1.90	1.6	Styrofoam 0.5	5.51	3.67	100
Argon 3	2.70	2.00	0.27	Styrofoam 0.3	5.09	3.83	59
Air	2.85	2.39	0.09	Xenon 5	5.15	4.43	6.4
<i>S</i> ₂ , <i>m</i> =1.25				Argon 100	5.05	4.08	34
Sample	3.98	1.76	635	Argon 80	5.19	4.21	29
Aluminum	7.88	1.89	401	Argon 50	5.44	4.45	20
Magnesium	7.26	2.19	280	Argon 20	5.54	4.55	8.3
Plexiglas	6.28	2.46	180	Argon 3	5.74	4.81	1.3
Styrofoam 0.5	4.84	3.16	76	Argon 1	6.38	5.17	0.6
Argon 30	4.35	3.40	7.3	Air	6.20	5.66	0.45
Argon 15	4.45	3.50	3.9				
Argon 3	4.53	3.67	0.8				
Air	4.50	4.00	0.23				

TABLE III. Parameters of the barriers used in the isentropic expansion method.

Barrier	ρ ₀ , g/cm ³	Limits of U, km/sec	C _{ba} , km/sec	λ _{ba}	Barrier	P ₀ , bar	Limits of U, km/sec	C _{ba} , km/sec	λ _{ba}
Aluminum	2.71	—	5.30	1.36	Xenon	5-30	3-12	0.10	1.14
Magnesium	1.74	—	4.49	1.26	"	1-3	3-12	0.10	1.10
Plexiglas	1.18	—	3.10	1.32	Argon	5-100	3-10	0.81	1.04
Polyethylene	0.92	—	2.83	1.48	"	1-3	3-10	0.75	1.03
Styrofoam	0.66	—	1.09	1.34	"	0,1-5	10-20	0.10	1.10
"	0.50	—	0.70	1.31	"	3-20	U<3		
"	0.30	—	0.15	1.29	Air	1	2-6	0.40	1.02
									Ideal gas

three terms

$$F(V, T) = E_x(V) + F_e(V, T) + F_r(V, T), \quad (2)$$

where *E_x* determines the "elastic" part of the interaction at *T* = 0 K, while *F_e* and *F_r* give the thermal contribution of the electrons and atoms. The terms *E_x* and *F_e* have the same form for the solid and liquid phases, while the forms of *F_r* are different.

The cold pressure *P_x* = -*dE_x*/*dV* at σ_k = *V*_{0k}/*V* > 1 (*V*_{0k} is the specific volume at *P* = 0 and *T* = 0 K) was specified in the traditional form³²

$$P_x(\sigma_k) = \sigma_k^{1/2} \sum_{i=1}^n a_i (\sigma_k^{1/3} - 1), \quad (3)$$

and σ_k < 1 in the form of a polynomial

$$P_x(\sigma_k) = [A(\sigma_k^m - 1) + B(\sigma_k^n - 1)]. \quad (4)$$

Both expressions satisfy the condition *P_x*(1) = 0; the coefficients in (3) and (4) are determined by the condition *dP_x*/*dσ_k* |_{σ_k=1} = *B*₀, and additionally for (4),

$$V_{0k} \int_1^{\sigma_k} \frac{P_x}{\sigma_k^2} d\sigma_k = E_s$$

(*B*₀ is the isothermal modulus of bulk compression at *T* = 0 K, calculated in accordance with Ref. 47, and *E_s* is the sublimation energy³³). The remaining leeway in the choice of coefficients *a_i* was used to reconcile the cold

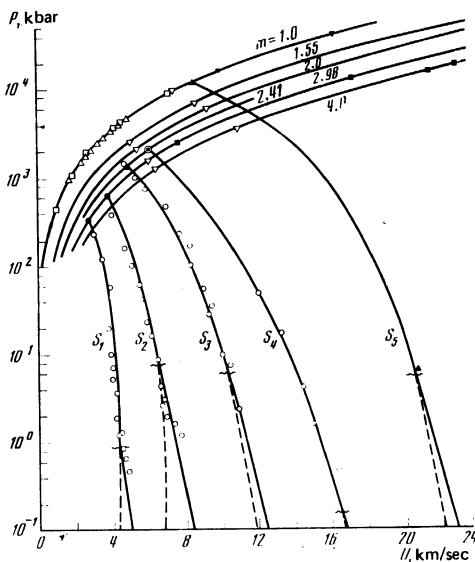


FIG. 4. *P*-*U* diagram of copper. Solid lines—calculation of expansion isentropes *S* and of shock adiabats for different porosities *m* (dashed—metastable adiabats within the two-phase region), ○—the authors' experiments on isentropic expansion ●—initial states on the shock adiabats), ▲—³⁹, shock-wave data: □—¹⁵, ▽—¹⁶, ▴—¹⁷, ■—¹⁹, △—⁴⁶.

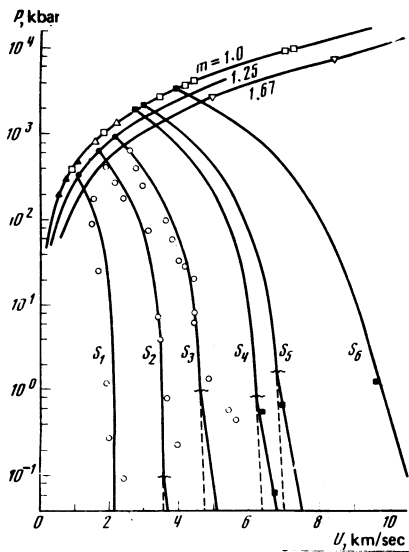


FIG. 5. $P-U$ diagram of lead. Notation the same as in Fig. 4, with the exception of \blacksquare — 22 , \blacktriangle — 44 , \triangle — 45 .

curve at $\sigma_k = 2-200$ interpolated according to Ref. 48 with the calculations by the Thomas-Fermi model, while the fit parameters m and n were used to obtain the experimental dependence of the density of the liquid phase of the metals on the temperature.^{49,50} The zero of the energy $E_x(V)$ in (2) was taken to be $E_x(V_{0k}) = 0$, and this determines the integration constants on going from P_x to E_x in (3) and (4).

The thermal part of the potential F_e is of the form

$$F_e(V, T) = -C_e(\sigma, T) T \ln \left[1 + \frac{B_e(T) T}{2C_{ei}} \sigma^{-\gamma_e(\sigma, T)} \right] \quad (5)$$

and contains generalized analogs of the coefficient of the electronic heat capacity B_e , of the electron Grüneisen coefficient γ_e , and of the heat capacity of the gas C_e , all of which depend on the temperature and on the degree of compression $\sigma = V_0/v$. Expression (5) should satisfy in the condensed phase the limiting relations

$$F_e(V, T) = -1/2 \beta_0 T^2 \sigma^{-\gamma_0}$$

for a degenerate electron gas at low temperatures and

$$F_e(V, T) = C_{ei} T \ln(\sigma^{2/3}/T)$$

for an ideal gas of electrons in the case of high temperatures ($C_{ei} = 3RZ/2$; R is the gas constant and Z is the atomic number of the element).

The Grüneisen coefficient of the electrons, with allowance for the asymptotic relations $\gamma_e = \gamma_0$ at $T = 0$ K and $\gamma_e = 2/3$ at $T \rightarrow \infty$, $\sigma = 0$, and $\sigma \rightarrow \infty$ is

$$\gamma_e(\sigma, T) = \frac{2}{3} + \left(\gamma_0 - \frac{2}{3} + \gamma_m \frac{T}{T_0} \right) \exp \left\{ -\frac{T}{T_0} - \frac{(\sigma - \sigma_m)^2}{\sigma \sigma_0} \right\}. \quad (6)$$

The term with γ_m makes it possible to take into account the anomalies in the temperature dependence of the Grüneisen coefficient at $\sigma \sim 1$. For the coefficient of the electronic heat capacity we chose the relation

$$\beta(T) = \beta_1 + \left(\beta_0 - \beta_1 + \beta_m \frac{T}{T_0} \right) \exp \left(-\frac{T}{T_0} \right), \quad (7)$$

which reflect its characteristic features,⁴ i.e., the existence of an extremum and of limiting values at low (β_0) and high (β_1) temperatures. Taking into account the

form of (7) for $\beta(T)$, we can determine

$$B_e(T) = \frac{2}{T^2} \int \left(\int \beta(\tau) d\tau \right) dT, \quad (8)$$

and in the case of constant β we have $B_e \equiv \beta$, while in a real situation we can obtain, by choosing the free parameters in (7), a sufficiently accurate description of the temperature dependence of $\beta(T)$.

The quantity $C_e(\sigma, T)$ in (5) tends at high temperatures to its limiting value C_{ei} , which characterizes an ideal electron gas. In the plasma region, the heat capacity should account for the effects of the first ionization and for the behavior of the ionized matter, and should approach smoothly C_{ei} . Taking these requirements into account, we chose for C_e the expression

$$C_e(\sigma, T) = \frac{3R}{2} \left[Z + \frac{\sigma_e T_e^2 (1-Z)}{(\sigma + \sigma_e)(T^2 + T_e^2)} \right] \exp \left(-\frac{\tau_i}{T} \right). \quad (9)$$

Here $\tau_i = T_i \exp(-\sigma/\sigma_i)$, where T_i is the value characteristic of the first ionization, while the exponential factor reflects the decrease of the ionization potential with increasing density.

The fit constants σ_e and T_e determine the characteristic density of the metal-vapor transition and the temperature of the transition from the singly ionized to the fully ionized gas.

The lattice component of the thermal part of the potential of the solid phase is given by

$$F_l^{(0)}(V, T) = 3RT \ln(\theta(\sigma)/T), \quad (10)$$

where θ/σ is the "effective" frequency, determined for a given cold curve from the experimental dependence of the Grüneisen coefficient $\gamma(\sigma) = d \ln \theta / d \ln \sigma$ on the degree of compression, which was taken with allowance for the asymptotic values $\gamma = 2/3$ at $\sigma = 0$ and $\sigma \rightarrow \infty$ in the form

$$\gamma(\sigma) = \frac{2}{3} + \frac{(\gamma_0 - 2/3)(B_s^2 + D_s^2)}{B_s^2 + (x + D_s)^2}, \quad (11)$$

where $x = \ln \sigma$, γ_0 is the Grüneisen coefficient under normal conditions, and B_s and D_s are fit coefficients. From the integration of (11) we obtain the frequency

$$\theta(\sigma) = \theta_0 \sigma^{\gamma_0} \exp \left\{ \frac{(\gamma_0 - 2/3)(B_s^2 + D_s^2)}{B_s} \left[\arctg \frac{x + D_s}{B_s} - \arctg \frac{D_s}{B_s} \right] \right\} \quad (12)$$

with an integration constant θ_0 determined from the entropy of the normal state. The sum of the cold, electronic, and lattice parts of the potential (3)-(12) determines completely the equation of state of the solid phase of the metal.

When metals are melted, a drastic transition takes place from the ordered structure of the lattice to the complete disorder of the nuclei at high temperatures. This leads to a change in both the spectrum of the oscillations and in the values of the specific heat in the course of melting and further heating, and these characteristics of the metal should be differently affected by the anharmonicity. If the oscillation spectrum can change drastically in the course of melting (a first-order phase transition), then the jump in the heat capacity due to the conservation of the short-range order in the liquid may not be so noticeable. The thermal contribution of the lattice nuclei to the potential of the liquid phase

$$F_r^{(0)}(V, T) = F_a(V, T) + F_m(V, T)$$

consists of two terms responsible for the anharmonicity effects. The first gives the spectrum of the oscillations and the heat capacity at sufficiently high temperatures ($T \gg T_m$, where T_m is the melting temperature at normal pressure), while the second determines directly the correct value of the jumps of the density and entropy in melting, the course of the melting curve, and the thermodynamics of the region close to the melting curve.

The potential F_a is given by an approximate equation similar to (10), but with a heat capacity that changes smoothly from the heat capacity of the lattice $3R$ to the heat capacity $3R/2$ of an ideal gas of nuclei. The Grüneisen coefficient tends in this case from its liquid value to the ideal-gas limit $2/3$. Taking this into account, we get for F_a

$$F_a(V, T) = \frac{3RT}{2} \left[1 + \frac{\sigma T_r}{(\sigma + \sigma_r)(T + T_r)} \right] \ln \frac{\theta_a(\sigma, T)}{T}, \quad (13)$$

where the values of σ_r and T_r determine the characteristic density and temperature of the transition to the heat capacity of an ideal gas.

The "frequency spectrum" is given by an expression for

$$\theta_a(\sigma, T) = T_{ca} \sigma^n \frac{\theta_1(\sigma) + T}{T_{ca} + T}, \quad (14)$$

where $\theta_1(\sigma)$ is determined by integrating the experimental dependence of the Grüneisen coefficient of the liquid phase on the density

$$\theta_1 = \exp \left\{ \int (\gamma_l - 2/\sigma) d \ln \sigma \right\},$$

with γ_l having a form similar to (11), and the integration constant θ_{01} determined from the condition $\theta_1(0) = T_{ca}$:

$$\theta_1(\sigma) = \theta_{01} \exp \left\{ \frac{(\gamma_{01} - 2/\sigma)(B_l^2 + D_l^2)}{B_l} \left[\arctg \frac{x + D_l}{B_l} - \arctg \frac{D_l}{B_l} \right] \right\}. \quad (15)$$

The potential term F_m should ensure the correct initial behavior of the melting curve, i.e., the specified entropy jump ΔS_m and volume jump ΔV_m at normal pressure, should attenuate strongly in the gas phase ($P_m \ll P_{com}$ and $E_m \ll E_{com}$ as $\sigma \rightarrow 0$), and decrease upon compression as a result of the elimination of the differences between the properties of the solid and liquid phases; at large degrees of compression $\gamma_{ml} = P_m V/E_m \rightarrow 2/3$. Taking into account the satisfaction of these requirements we have

$$F_m(V, T) = 3R \left\{ \frac{2\sigma_{ml} T_m \sigma^2}{\sigma^2 + \sigma_{ml}^2} \left[C_m + \frac{3A_m}{5} \left(\left(\frac{\sigma}{\sigma_{ml}} \right)^{1/2} - 1 \right) + (B_m - C_m) T \right] \right\}, \quad (16)$$

where σ_{ml} is the relative density of the liquid phase at $P = 1$ bar; the constants A_m , B_m , and C_m are determined uniquely from the phase-equality condition:

$$P^{(l)} = P^{(s)} = \bar{P}, \quad S^{(l)} = S^{(s)} + \Delta S_m, \quad F^{(l)} = F^{(s)} + \bar{P} \Delta V_m.$$

The combination (2)–(16) specifies completely the thermodynamic potential of the metals on the entire phase plane. The action of each free parameter in the formulas is localized to a sufficient degree and, for example, a change of an β_m and β_l in (7) influences the thermodynamics of the condensed phase at low temperatures, but has no effect whatever in the plasma region,

where the important role is played by the constants T_i and T_c which are determined by the condition for the description of the first ionization and the transition from the plasma to an ideal electron gas. The free constants in (3)–(16) for the equations of state of copper and lead were chosen from the condition that they duplicate (within the limit of the accuracy of the initial information) the results of the static and dynamic experiments and of calculations in accordance with the theoretical model.

4. DISCUSSION OF RESULTS AND CONCLUSIONS

On the basis of the experimental results and of additional thermodynamic information we determined the coefficients of the equations of state of copper and lead, which are given in Table IV. Figures 4 and 5 give the calculated the metastable and equilibrium release isentropes and the shock adiabats for different porosities. A comparison of the calculated isentropes with the experimental data shows that at pressures above critical the maximum discrepancies in the expansion rates amount to 3–4%, a value at the limit of the experimental error. On entering the two-phase region, an increase is observed in the deviation of the calculated curves from the experimental results; this is possibly due to the non-uniform distribution of the energy in the heated particles of the metal. This is indicated by the decrease of the difference between the experiment and calculation with increasing entropy, which improves the particle-heating conditions. The agreement of the calculation with the experimental results on the release in air of shock-compressed solid samples of copper³⁹ and lead²² confirms the assumption that the increased expansion rate of the porous samples above the corresponding calculated values, observed at low pressures, is due to their uneven heating.

From the conversion of the experimental curves into thermodynamic variables in accordance with relation (1), it follows that in the course of expansion we were able to cover an exceedingly wide range of parameters—four decades in pressure and two in density—from a strongly compressed metallic liquid to a quasi-ideal Boltzmann plasma and metallic vapor. The electron de-

TABLE IV. Coefficients of equations of state of copper and lead.

V_0	V_{0h}	R	Z	T_m	σ_{ml}	A_m	B_m	C_m
0.112	0.110	0.13	29	1.360	0.895	1.00	-5.13	0.24
0.0882	0.0860	0.04	82	0.602	0.930	2.16	-5.28	0.20
a_1	a_2	a_3^*	a_4^*	a_5^*	A	B	m^*	n^*
5863.61	-7653.82	6356.76	-870.84	60.11	13.6	38.8	8	0.1
-913.00	514.10	2.17	8.27	0	4.16	24.92	10	0.4
γ_0^*	γ_m^*	σ_m^*	σ_l^*	T_g^*	β_0	β_l^*	β_m^*	T_b^*
0.4	1.4	1.0	2.5	300	0.0109	0.0141	0.04	5.0
0.9	-0.5	6.0	8.0	1000	0.0144	0.0098	0	5.0
σ_r^*	T_r^*	σ_r^*	T_r^*	σ_r^*	T_r^*	T_{ca}^*	T_{ca}^*	
0.3	40	0.5	200	0.03	80	14	40	
0.3	20	0.1	200	0.05	40	4	30	
γ_0	B_l^*	D_l^*	0_0	γ_{01}^*	B_l^*	D_l^*	0_{01}	
1.96	1.0	0.10	0.22	1.6	0.66	-0.64	211	
2.73	0.9	0.10	0.058	1.6	0.8	-0.47	85	

Note. The upper and lower coefficients pertain to the equations of state of copper and lead, respectively. The units of the measurement of the coefficients correspond to the initial units— $E = 10^{10}$ erg/g, $V = 1$ cm³/g, and $T = 10^3$ K. Thus, for example, $\beta_0 = E/T_c^2 = 10^4$ erg/g · K², etc. The fit parameters are marked in the table with an asterisk.

generacy is lifted, the electron energy spectrum is radically restructured, partial recombination of a dense plasma is realized, a metal-insulator transition takes place in an electronic disordered structure, and a plasma that is non-ideal with respect to various types of interparticle interaction is produced.

The presence of strong collective interaction makes a consistent theoretical description of the properties of matter difficult, and we propose here only a number of realistic models,^{5,23-26} that characterize individual effects in relatively limited parts of the phase diagram. The principal qualitative result of most models is an indication of a possible loss of thermodynamic stability and stratification of a strongly non-ideal plasma into new exotic phases, something that would distort substantially the usual form of the phase diagram of a metal. Our experiments have shown absence of any noticeable jumps in the thermodynamic functions or of any hydrodynamic anomalies that might be interpreted as specific plasma phase transformations. The data of Tables I and II and of Figs. 4 and 5 point to a continuous variation of the properties of the metals as they expand from the condensed to the gaseous state. We emphasize that the discussed phase anomalies are most probable precisely in the investigated range of parameters, since an increase of the temperature and a decrease of the density lead to a relative decrease of the effects of deviation from the ideal state.

Figures 6 and 7 show that P - ρ phase planes of copper and lead, on which are marked the shock adiabats for different porosities. The traditional region of shock-wave research, limited to pressures ~ 10 Mbar, is described by the obtained equations of state, as shown by the figure, with high accuracy. The experiment is adequately described both with respect to the shock-

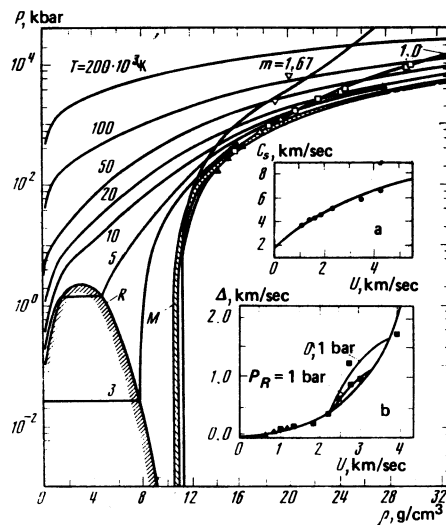


FIG. 7. P - ρ phase plane of lead. Notation the same as in Fig. 6, with the exception of Δ —⁴⁴, Δ —⁴⁵; a) The same as in Fig. 6a for lead; b) Deviation from the rule of doubling of the velocities when lead relaxes in air, $\Delta = W - 2U$, \blacksquare —²².

wave excitation of the pressure and density and with respect to the measurements of the speed of sound in shock-compressed metals⁵² (Figs. 6a and 7a). The determination, with the aid of the equations of state, of the temperature and entropy (as well as of the position of the melting curve) at high pressures in the condensed-phase region is usually based on a plausible extrapolation of the properties of the metal under normal conditions to regular asymptotic values.^{15,16,32,33} In the derived equations of state, the values of the temperature and of the entropy of the condensed phase of copper and lead are quite definitely established through the use of results obtained on isentropic expansion in the present and other studies.^{20,22}

The release isentropes (see Fig. 1) connect phase-plane sections that differ radically both in the physical state of the metal and in the character of the initial experimental information. When the entire phase plane is described by a single thermodynamic potential, the expansion isentropes serve as a unique closing link for the equations of state, since they connect the shock-wave and near-critical states of equal entropy, and furthermore, when the two-phase liquid-vapor region is reached they have volume and energy values that agree with the parameters of the equilibrium line.

The melting curves of copper⁵³ and lead⁵⁴ were experimentally investigated in the pressure interval up to 50 kbar: the calculated values $T_m(P)$ agreed fully with experiment. Limited information on the melting curve of copper in the high-pressure region was obtained from measurements²⁰ of the residual temperature following expansion of shock-compressed samples (Fig. 6b). This method revealed on the shock adiabat an interval from 1.4 to 1.8 Mbar corresponding to the enthalpies of the start and end of the melting of a metal relaxed to the normal pressure. Because of the increase of the entropy on the $T_m(P)$ curve, the melting on the Hugoniot adiabat is shifted towards larger entropies and corresponds to pressures 1.9–2.7 Mbar ac-

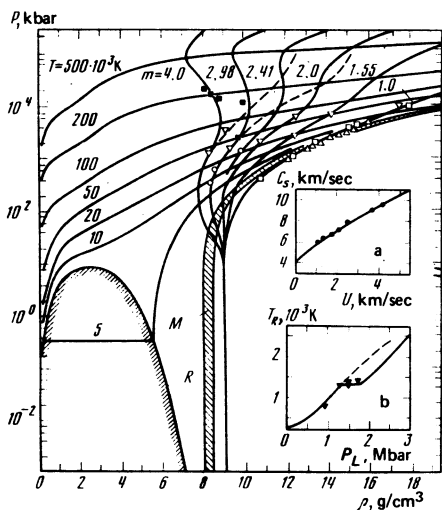


FIG. 6. P - ρ phase plane of copper: M —melting region, R —liquid-vapor equilibrium curve, T —isotherms, m —shock adiabats for different porosities. Shock-wave data: \circ —authors' experiments, \square —¹⁵, ∇ —¹⁶, \blacksquare —¹⁹, Δ —⁴⁶. Dashed—interpolation of shock adiabats to TFC model calculations⁵¹. a) Dependence of the speed of sound C_s on the shock adiabat of copper on the mass velocity of the shock wave U ; \bullet —⁵². b) Dependence of the residual temperature of copper T_R in the case of relaxation in air from the initial pressure in the shock wave P_H ; \blacktriangledown —²⁰, dashed—calculation¹⁰ without allowance for melting.

ording to calculations using the equation of state. The calculation of the residual temperatures at lower pressures agrees with good accuracy with the results of the experiment.²⁰ As seen from Fig. 6b, calculation¹⁰ carried out without allowance for the melting yields residual temperatures that are 500 K too high.

The pressure corresponding to the melting of lead in shock waves was determined experimentally (see the review⁵⁵) on the basis of the following criteria: the change of the form of the crater upon penetration of an aluminum disk (220 kbar), the shapes of the cumulative ejecta (230–250 kbar), the decrease of the viscosity (410 kbar), and the break in the linear $D-U$ plot (280 kbar). In a preceding paper²² the melting was associated with the deformation of the curve $\Delta(U) = W - 2U$, which characterizes the violation of the rule of velocity doubling in release (U is the mass velocity in the shock wave and W is the rate of spreading in air). The $\Delta(U)$ curve calculated for lead from the obtained equation of state describes satisfactorily the results of the expansion experiments (Fig. 7b) and corresponds to melting on the shock adiabat in an interval 300–460 kbar. We note that the melting curves obtained here for copper and lead and for the points of their intersection with the shock adiabats are close to the results of calculations based on the equation of state of the condensed phase.³³

The properties of liquid metals are determined on the basis of the results of experimental measurements of the enthalpy and density at normal pressure.^{8, 49, 50} For lead, additional measurements of these quantities were made at a pressure $P = 3$ kbar up to near-critical temperature by the exploding-wire method.¹³ The accuracy with which the experiments aimed at determining the density of the liquid phase of copper and lead are described is demonstrated in Figs. 8a and 8b, which show the calculated plots of the density against temperature on the isobars, as well as the liquid-vapor equilibrium lines. The information on the critical parameters of most metals, including copper and lead, is available in the form of semi-empirical estimates,^{38, 56–58} which are also plotted in the figures. The calculated parameters of the critical points are close to the estimates of ρ_c , T_c , and P_c ; on the lowest segments (up to $T \sim 0.7T_c$) of the phase-equilibrium line the logarithm of the pressure is a linear function of the reciprocal temperature.¹¹ Figures 8a and 8b show also the deviations from the rule that the diameter of the calculated function $\bar{\rho}(T) = (\rho_L + \rho_G)/2$ be a linear function (ρ_L is the density of the liquid and ρ_G is the density of the gas). We note that in contrast to alkali metals, for which the linear-diameter rule is well satisfied, a similar excess density on the $\bar{\rho}(T)$ curve was observed experimentally for mercury.¹² The calculation yielded the following critical parameters for copper:

$$P_c = 9.07 \text{ kbar}, \quad T_c = 7830 \text{ K} \quad V_c = 0.47 \text{ cm}^3/\text{g} \quad S_c = 1.97 \text{ J}/(\text{gK}),$$

and for lead:

$$P_c = 2.37 \text{ kbar}, \quad T_c = 5530 \text{ K} \quad V_c = 0.32 \text{ cm}^3/\text{g} \quad S_c = 0.56 \text{ J}/(\text{gK}).$$

The variation of the thermodynamic characteristics on the liquid-vapor phase-equilibrium line is shown on the $P-S$ and $\rho-T$ diagrams in Figs. 3 and 8.

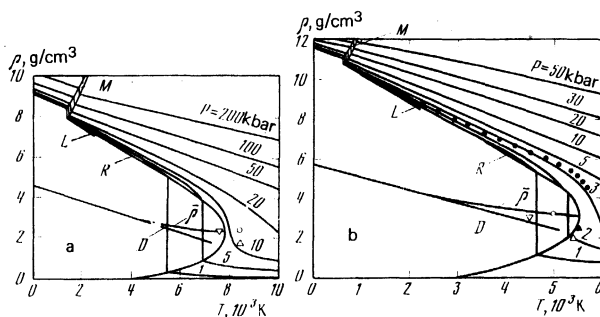


FIG. 8. Region of low pressures in the condensed phase of copper (a) and lead (b): M —melting curve, R —liquid-vapor equilibrium line, D —linear diameter, $\bar{\rho}(T) = (\rho_L + \rho_G)/2$, P —isobars, L —density of liquid metal at $P = 1$ bar for copper⁴⁹ and lead.⁵⁰ Estimates of the critical-point parameters: \circ —³⁸, \triangle —⁵⁶, \triangleleft —⁵⁷, \triangle —⁵⁸; \bullet —measurement of the density of liquid lead at $P = 3$ kbar.¹³

The relative positions of the continuous shock adiabats at $P = 15$ –50 Mbar,¹⁹ the final states correspond, in contrast to compression of non-porous samples, to a weakly degenerate electron gas with unusually high concentration of the thermal energy, $\sim 3 \times 10^3$ kJ/cm³. According to the TFC model⁵¹ these conditions correspond to characteristic values ~ 0.45 of the Grüneisen coefficient of the electrons, which lead to high degrees of compression under shock loading (dashed curve in Fig. 6). This result patently contradicts the experimental results of Zubarev *et al.*¹⁹ on the compressibility of porous samples of copper, which are shown in the same figure, and lead to an electron Grüneisen coefficient 0.7–0.8. Some uncertainty in the position of the shock adiabat of aluminum, relative to which the states of copper were determined, is much smaller than the observed discrepancy and cannot account for it. This is evidence that the TFC model is not applicable to the indicated experimental region and that it is necessary to resort to calculation methods that take explicit account of the concrete shell structure of the element.

An alternate model that explains the unique course of the shock adiabats of porous copper may be the model of a multicomponent, partially degenerate nonideal plasma. In fact, the ratio of the average electrostatic energy of the Coulomb interaction to the average kinetic energy of the plasma $\Gamma = e^2/kTr_D [r_D = (kT/4\pi e^2 \sum n_e Z^2)^{1/2}$ is the Debye screening radius] at $\rho \sim \rho_0$ and $T \sim 10^5$ K is equal to 1–3, so that it becomes possible to take into account the effects of interparticle Coulomb interaction within the framework of an asymptotic perturbation theory (the annular Debye approximation in a ground canonical ensemble of statistical mechanics⁴²). The limits of applicability of this approach were established earlier by experiments on shock compression of Cs, Ar, and Xe.^{43, 41} A realistic determination of the thermodynamic properties of a weakly degenerate metal was obtained with the aid of the model of the “bounded” atom, which takes explicit account of the effects of ionization and the characteristic dimension of the ions. Selected calculations yielded the experimental values of the Grüneisen coefficients; the thermodynamics of these calculations is close to the results of the description of the experimental region by the plotted interpolation equation of

state.

A comparison of the results of the calculations of the characteristics of copper and lead from the equations of state of the present paper and from the available experimental and calculated data demonstrates the feasibility of an adequate thermodynamic description on the entire phase plane. This will make possible an extensive use of the developed equations of state in concrete calculations.

The authors thank A. N. Dremin for constant interest and help, G. M. Gandel'man and I. I. Sharipdzhanov for helpful discussions, and V. K. Gryaznov for the plasma calculations.

¹We note that a similarly undervalued compressibility was observed in dynamic compression of a cesium plasma,⁴³ apparently due to deformation of the discrete spectrum of the dense plasma.

¹P. Caldirola and H. Knoepfel, eds., *Physics of High Energy Density*, Academic, 1971.

²D. A. Kirzhnits, Yu. E. Lozovik, and G. V. Shpatakovskaya, *Usp. Fiz. Nauk* 117, 3 (1975) [Sov. Phys. Usp. 18, 649 (1975)].

³A. A. Vedenov and A. I. Larkin, *Zh. Eksp. Teor. Fiz.* 36, 1133 (1959) [Sov. Phys. JETP 9, 806 (1959)].

⁴A. I. Voropinov, G. M. Gandel'man, and V. G. Podval'nyi, *Usp. Fiz. Nauk* 100, 193 (1970) [Sov. Phys. Usp. 13, 56 (1970)]. G. M. Gandel'man, Doctoral Dissertation, Inst. Phys. Prob., 1966.

⁵V. M. Zamalin, G. E. Norman, and V. S. Filinov, *Metod Monte-Karlo v statisticheskoi fizike (Monte Carlo Method in Statistical Physics)*, Nauka, 1976.

⁶N. F. Carnahan and K. E. Starling, *J. Chem. Phys.* 51, 635 (1969). W. G. Hoover, M. Ross, K. W. Johnson, D. Henderson, J. A. Barker, and B. C. Brown, *J. Chem. Phys.* 52, 4931 (1970).

⁷E. Yu. Tonkov, *Fazovye diagrammy élementov pri vysokom davlenii (Phase Diagrams of Elements at High Pressure)*, Nauka, 1979.

⁸R. Hultgren, P. D. Desai, and D. T. Hawkins, *Selected Values of the Thermodynamic Properties of the Elements*, Metal Park, 1973; *Handbook of Chemistry and Physics*, ed. by R. C. Weast, Cleveland, 1975.

⁹H. K. Mao, P. M. Bell, J. W. Shaner, and D. J. Steinberg, *J. Appl. Phys.* 49, 3276 (1978).

¹⁰R. G. McQueen, S. P. Marsh, J. W. Taylor, J. N. Fritz, and W. J. Carter, in: *High Velocity Impact Phenomena*, ed. by R. Kinslow, N.Y., 1970, p. 293.

¹¹R. G. Ross and D. A. Greenwood, *Prog. Mater. Sci.* 14, 173 (1971).

¹²V. A. Alekseev, A. A. Andreev, and V. Ya. Prokhorenko, *Usp. Fiz. Nauk* 106, 393 (1972) [Sov. Phys. Usp. 15, 139 (1972)].

¹³J. W. Shaner and G. R. Gathers, UCRL-79586, Livermore, 1977; *Proc. of Seventh Symp. on Thermophysical Properties*, Gaithersburg, 1977.

¹⁴L. V. Al'tshuler, *Usp. Fiz. Nauk* 85, 197 (1965) [Sov. Phys. Usp. 8, 52 (1965)].

¹⁵L. V. Al'tshuler, S. B. Kormer, A. A. Bakanova, and R. F. Trunin, *Zh. Eksp. Teor. Fiz.* 38, 790 (1960) [Sov. Phys. JETP 11, 573 (1960)]. L. V. Al'tshuler, A. A. Bakanova, and R. F. Trunin, *Zh. Eksp. Teor. Fiz.* 42, 91 (1962) [Sov. Phys. JETP 15, 65 (1962)].

¹⁶S. B. Kormer, A. I. Funtikov, V. D. Urlin, and A. N. Kolesnikova, *Zh. Eksp. Teor. Fiz.* 42, 686 (1962) [Sov. Phys. JETP 15, 477 (1962)].

¹⁷L. V. Al'tshuler, B. N. Moiseev, L. V. Popov, G. V. Sim-

akov, and R. F. Trunin, *Zh. Eksp. Teor. Fiz.* 54, 785 (1968) [Sov. Phys. JETP 27, 420 (1968)]. R. F. Trunin, M. A. Podurets, B. N. Moiseev, G. V. Simakov, and L. V. Popov, *Zh. Eksp. Teor. Fiz.* 56, 1172 (1969) [Sov. Phys. JETP 29, 630 (1969)]. R. F. Trunin, M. A. Podurets, G. V. Simakov, L. V. Popov, and B. N. Moiseev, *Zh. Eksp. Teor. Fiz.* 62, 1043 (1972) [Sov. Phys. JETP 35, 550 (1972)].

¹⁸C. E. Ragan III, M. G. Silbert, and B. C. Diven, *J. Appl. Phys.* 48, 2860 (1977).

¹⁹V. N. Zubarev, M. A. Podurets, L. V. Popov, G. V. Simakov, and R. F. Trunin, in: *Detonatsiya (Detonation)*, Chernogolovka, Joint Inst. of Chem. Phys., 1978, p. 61.

²⁰J. W. Taylor, *J. Appl. Phys.* 34, 2727 (1963).

²¹K. Hornung and K. W. Michel, *J. Chem. Phys.* 56, 2072 (1972).

²²L. V. Al'tshuler, A. A. Bakanova, A. V. Bushman, I. P. Dudoladov, and V. N. Zubarev, *Zh. Eksp. Teor. Fiz.* 73, 1866 (1977) [Sov. Phys. JETP 46, 980 (1977)].

²³Ya. B. Zel'dovich and L. D. Landau, *Zh. Eksp. Teor. Fiz.* 14, 32 (1944).

²⁴G. E. Norman and A. N. Starostin, *Teplofiz. Vys. Temp.* 8, 413 (1970).

²⁵I. T. Yakubov, *Zh. Eksp. Teor. Fiz.* 58, 2075 (1970) [Sov. Phys. JETP 31, 1118 (1970)].

²⁶Z. G. Khrapak and I. T. Yakubov, *Zh. Eksp. Teor. Fiz.* 59, 945 (1970) [Sov. Phys. JETP 32, 514 (1970)].

²⁷Ya. B. Zel'dovich and Yu. P. Raizer, *Fizika udarnykh voln i vysokotemperaturnykh gidrodinamicheskikh yavlenii (Physics of Shock Waves and High-Temperature Hydrodynamic Phenomena)*, Nauka, 1966 [Academic Press].

²⁸I. C. Skidmore and E. Morris, *Proc. of Symp. on Thermodynamics of Nuclear Materials*, IAEA, Vienna, 1962, p. 173.

²⁹Yu. L. Alekseev, V. P. Ratnikov, and A. P. Rybakov, *Zh. Prikl. Mekh. Tekh. Fiz. No. 2*, 101 (1971).

³⁰B. L. Glushak, M. V. Zhernokletov, and V. N. Zubarev, *Papers of All-Union Symp. on Pulsed Pressures*, Vol. 1, VNIIFTRI, 1974, p. 87.

³¹V. E. Fortov, A. A. Leont'ev, A. N. Dremin, and S. V. Pershin, *Pis'ma Zh. Eksp. Teor. Fiz.* 20, 30 (1974) [JETP Lett. 20, 13 (1974)]; in *Gorenie i vzryv (Combustion and Explosion)*, Nauka, 1977, p. 515.

³²S. B. Kormer and V. D. Urlin, *Dokl. Akad. Nauk SSSR* 131, 542 (1960) [Sov. Phys. Dokl. 5, 317 (1960)]. S. B. Kormer, V. D. Urlin, and L. T. Popova, *Fiz. Tverd. Tela (Leningrad)* 3, 2131 (1961) [Sov. Phys. Solid State 3, 1547 (1962)].

³³V. D. Urlin, *Zh. Eksp. Teor. Fiz.* 49, 485 (1965) [Sov. Phys. JETP 22, 341 (1965)].

³⁴E. B. Royce, UCRL-51121, Livermore, 1971. D. A. Young, UCRL-51575, Livermore, 1974.

³⁵C. Boissière and G. Fiorese, *Rev. Phys. Appl.* 12, 857 (1977).

³⁶A. V. Bushman, V. E. Fortov, and I. I. Sharipdzhanov, *Teplofiz. Vys. Temp.* 15, 1095 (1977). L. V. Al'tshuler, A. V. Bushman, and B. S. Chekin, in: *Metrologiya bystroprotektayushchikh protsessov (Metrology of High-Speed Processes)*, Moscow, VNIIFTRI, 1977, p. 4.

³⁷V. E. Fortov and A. A. Leont'ev, *Zh. Prikl. Mekh. Tekh. Fiz. No. 3*, 162 (1974).

³⁸V. E. Fortov, A. N. Dremin, and A. A. Leont'ev, *Teplofiz. Vys. Temp.* 13, 1072 (1975).

³⁹Ph. De Beaumont and J. Léyonie, *Proc. of Fifth Symp. on Detonation*, Pasadena, 1970, p. 430.

⁴⁰L. V. Al'tshuler and I. I. Sharipdzhanov, *Fiz. Zemli No. 3*, 11 (1971).

⁴¹V. K. Gryaznov, M. V. Zhernokletov, V. N. Zubarev, I. L. Iosilevskii, and V. E. Fortov, *Zh. Eksp. Teor. Fiz.* in press [Sov. Phys. JETP].

⁴²V. K. Gryaznov, I. L. Iosilevskii, and V. E. Fortov, *Zh. Prikl. Mekh. Tekh. Fiz. No. 3*, 70 (1973).

⁴³A. V. Bushman, B. N. Lomakin, V. A. Sechenov, V. E. Fortov, O. E. Shchekotov, and I. I. Sharipdzhanov, *Zh. Eksp. Teor. Fiz.* 69, 1624 (1975) [Sov. Phys. JETP 42, 828 (1975)].

- ⁴⁴J. M. Walsh, M. H. Rice, R. G. McQueen, and F. L. Yarger, *Phys. Rev.* **108**, 169 (1957).
- ⁴⁵R. G. McQueen and S. P. Marsh, *J. Appl. Phys.* **31**, 1253 (1960).
- ⁴⁶W. M. Isbell, F. H. Shipman, and A. H. Jones, Hugoniot equation of state measurements for eleven materials to five megabars, *Mater. Sci. Lab. Rep. MSL-68-13*, 1968.
- ⁴⁷M. W. Guinan and D. J. Steinberg, *J. Phys. Chem. Solids* **35**, 1501 (1974).
- ⁴⁸N. N. Kalitkin and I. A. Govorukhina, *Fiz. Tverd. Tela (Leningrad)* **7**, 355 (1965) [*Sov. Phys. Solid State* **7**, 287 (1965)].
- ⁴⁹J. A. Cahill and A. D. Kirshenbaum, *J. Phys. Chem.* **66**, 1080 (1962).
- ⁵⁰A. D. Kirshenbaum, J. A. Cahill, and A. V. Grosse, *J. Inorg. Nucl. Chem.* **22**, 33 (1961).
- ⁵¹N. N. Kalitkin, L. V. Kuz'mina, and G. V. Shpatakovskaya, *Teplofiz. Vys. Temp.* **15**, 186 (1977). N. N. Kalitkin and L. V. Kuz'mina, Preprint Inst. Appl. Mech. No. 14, 1976.
- ⁵²L. V. Al'tshuler, S. B. Korner, M. I. Brazhnik, L. A. Vladimirov, M. P. Speranskaya, and A. I. Funtikov, *Zh. Eksp. Teor. Fiz.* **38**, 1061 (1960) [*Sov. Phys. JETP* **11**, 766 (1960)].
- ⁵³J. Akella and G. C. Kennedy, *J. Geophys. Res.* **76**, 4969 (1971).
- ⁵⁴P. H. Mirwald and G. C. Kennedy, *J. Phys. Chem. Solids* **37**, 795 (1976).
- ⁵⁵G. E. Duvall and R. A. Graham, *Rev. Mod. Phys.* **49**, 523 (1977).
- ⁵⁶E. Morris, AWRE Report 0-67/64, London, UKAEA, 1964.
- ⁵⁷D. A. Young and B. J. Alder, *Phys. Rev. A* **3**, 364 (1971).
- ⁵⁸K. Hornung, *J. Appl. Phys.* **46**, 2548 (1975).

Translated by J. G. Adashko

Dynamics of domain walls in weakly ferromagnetic orthoferrites

M. V. Chetkin and A. I. Akhutkina

M. V. Lomonosov Moscow State University

(Submitted 25 July 1979)

Zh. Eksp. Teor. Fiz. **78**, 761-766 (February 1980)

The velocity of domain walls in mechanically and chemically polished plates of YFeO_3 is investigated in large pulsed fields at 293 and 100 K. The velocity was determined from the time of passage of the wall over a given distance between two light spots. It is shown that after attainment of a limiting velocity equal to $2 \cdot 10^6$ cm/sec and corresponding to the minimum velocity of spin waves, there occurs a rapid increase of velocity to $2 \cdot 10^7$ cm/sec. The increase of velocity begins sooner, the more strongly the moving wall interacts with the unavoidable defects at the surface of the plate. In a mechanically polished specimen, the increase of velocity begins in fields of 0.7 kOe; in chemically polished, at fields larger than 3 kOe. In a mechanically polished YFeO_3 plate, at the back edge of the light pulse obtained on reverse motion of the wall through the light spots there occurs an instability that indicates a transition from stationary motion to turbulent. The instability appears after the wall attains the limiting velocity.

PACS numbers: 75.70.Kw, 81.40.Rs, 81.60. - j

1. INTRODUCTION

The limiting velocity of a domain wall in weakly ferromagnetic orthoferrites was first measured experimentally in work of one of the authors.¹ In yttrium orthoferrite, this velocity is $2 \cdot 10^6$ cm/sec and corresponds to the minimum phase velocity of spin waves with limiting wave vectors.² A solution of the Walker type for a weak ferromagnet was obtained by Zvezdin.³ Limiting velocities of domain walls have been attained experimentally in pulsed magnetic fields H_p of order of magnitude 1000 Oe. This is much lower than theory predicts.³ On further increase of H_p , the domain-wall velocity again increases and exceeds the limiting velocity by an order of magnitude. It was first pointed out in a paper of one of the authors⁴ that the region of constancy of the limiting wall velocity with respect to magnetic field must be finite, as occurs in interaction of a moving domain wall with sound. Above-limit velocities of a domain wall were first observed in YFeO_3 at room temperature in Ref. 5.

The present paper presents results of investigations

of motion of domain walls in weakly ferromagnetic orthoferrites with above-limit velocities. The investigations were made at 293 and 100 K for two types of walls in YFeO_3 specimens, whose surfaces were polished mechanically and chemically.

2. METHOD OF INVESTIGATION

The velocity of the domain wall was determined, by means of the dynamic Faraday effect, from the measured time of passage over a given distance between two light spots. The method of investigation that we used has been described in Ref. 4.

For production of the pulsed magnetic field, two coils were used, of diameter 1-1.5 mm corresponding to 7-14 turns, fastened from the two sides on to the surfaces of the plates of the orthoferrites under study. At the input of an electron multiplier FÉU-30, in order to diminish the noise, a diaphragm was placed, which transmitted only the two light beams obtained from the two light spots focused on to the plate. The minimum time of passage of a domain wall over a distance of 540 μm ,